

Article

# Use of Stirling Engine for Waste Heat Recovery

Peter Durcansky \* , Radovan Nosek  and Jozef Jandacka

Department of Power Engineering, Faculty of Mechanical Engineering, University of Zilina, 010 26 Zilina, Slovakia; radovan.nosek@fstroj.uniza.sk (R.N.); jozef.jandacka@fstroj.uniza.sk (J.J.)

\* Correspondence: peter.durcansky@fstroj.uniza.sk

Received: 2 June 2020; Accepted: 4 August 2020; Published: 10 August 2020



**Abstract:** Even though this discovery dates back to 1816, the greatest advancement in technology and understanding of Stirling-cycle devices has occurred in the last 50 years. Although their mass production is currently limited to special-purpose machines, its prospective use is in combination with renewable sources and indicates a potential for commercial purposes. The lack of commercial success, despite obvious advantages, is probably due to a lack of appropriate modeling techniques and theoretical predictions of what these devices can achieve. Nowadays the Stirling engine has found its use mainly in solar power plants, where it represents the only piston engine converting solar energy into mechanical and then electricity with relatively high efficiency. The Stirling engine also appears to be suitable for recovering waste heat, especially in heavy industry. The numerical model was adapted for the existing Cleanergy Stirling engine, to evaluate the possibilities of this one engine for waste heat recovery. This paper also deals with application options and individual parameters that affect the efficiency of this Stirling engine for waste heat recovery. The analysis showed that this kind of engine is capable of recovering and utilizing heat above 300 °C, which determines its possible use with solar energy.

**Keywords:** waste heat; Stirling engine; heat recovery

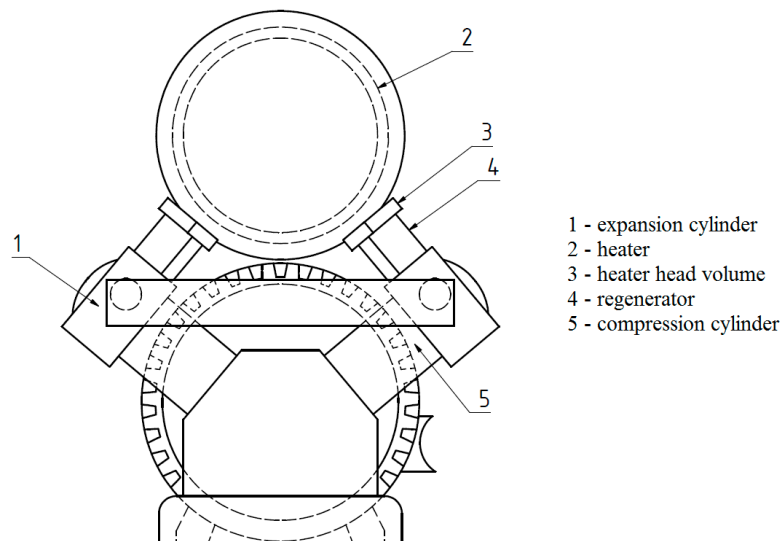
## 1. Introduction

A Stirling engine is one of the few representatives of hot-air engines. At the time of invention, its efficiency was comparable to the steam engine. This engine forms a closed thermodynamic system, using heat energy supplied from an external source and converts it to mechanical [1]. Its construction consists of two pistons and one or two cylinders, with a regenerator placed between. A regenerator can be used as a wire or ceramic grid, or any kind of porous material, which has a high heat capacity and low thermal conductivity. The regenerator serves for the temporary storage of thermal energy [2]. A great advantage of the Stirling engine, but also other hot air engines, is the variety of heat sources that can be used [3]. The simpler design compared to internal combustion engines with only a few moving parts is a great advantage. Single-phase working medium, without production of any carbon fouling, allows an extended service interval. Very low noise, smooth operation and low vibration level make these engines also suitable for domestic use. The engine does not necessary need oxygen for burning process, where the heat can be supplied from any heat source, allowing its use in space applications. One of the best described engines is the GM GPU3 Stirling engine, which served as the basis for many projects. This engine has 236 cm<sup>3</sup>, rhombic drive, and works with pressure from 1.2 to 6.9 MPa [4,5]. The impact of the working medium is very significant, but no less important is the regenerator located between the two cylinders, where heat is transferred from the hot to the cold cylinder, which should be supplied to the medium during further isochoric compression [6]. As working medium can be used air, but the most common is helium [7]. A comparison to other engines and some new models is shown in Table 1. This table presents engines prepared for production, but also experimental engines. The most suitable experimental engines for heat recovery are those with lower heater temperatures [7].

**Table 1.** List of Stirling engines.

Engine Manufacturer	Mean Pressure (MPa)	Heater Temperature (°C)	Power (kW)	Efficiency (%)
United Stirling [8]	14.5	691	35	30
Philips [7]	14.2	649	23	38
GM GPU-3 [8]	Up to 6.9	816	8.1	39
Farwell [8]	0.1	594	0.1	16.9
Karabulut et al. [9]	0.4	260	0.183	N/A
Kwankaomeng [10]	0.1	150	0.1	5.6
Cooke-Yarborough [11]	N/A	292	0.107	13.7
Solo Stirling [12]	N/A	Min. 540	7.3	25.4
WhisperGen [wikipedia]	N/A	Min. 550	Up to 1 kW	11
Viessmann Vitotwin [viessmann.de]	N/A	Min. 500	Up to 1 kW	30
Cleanergy [12]	1.5–9	N/A	2–9	25

Our laboratory is working with the Cleanergy Stirling engine, so to analyze and evaluate the properties of this Stirling engine for application in the heat recovery system, we have chosen to evolve a numerical model. The engine is  $\alpha$ -type, with 160 cm<sup>3</sup>, and the cross-section is shown in Figure 1. The aim of this work is to give information from experiments with this commercially available engine under various conditions and its capability for the heat recovery system.

**Figure 1.** Cleanergy  $\alpha$ -type Stirling engine, adaptation from [11].

## 2. Numerical Model

Stirling engine cycle is composed of isothermal compression, expansion, constant volume heating, and cooling [12]. One of the first analyses of the Stirling engine is the Schmidt analysis, made by Gustaf Schmidt in 1871 [13]. He made some assumptions, for example, all parts are moving sinusoidally, constant temperatures in all parts of the engine, and perfect gas law is applied to working fluids. Input parameters for application engines according to Schmidt analyses are the volumes  $V_{swe}$ ,  $V_{cle}$ ,  $V_r$ ,  $V_{swc}$ ,  $V_{clc}$  working temperatures  $T_h$ ,  $T_k$ , as shown in Figure 2 [12].

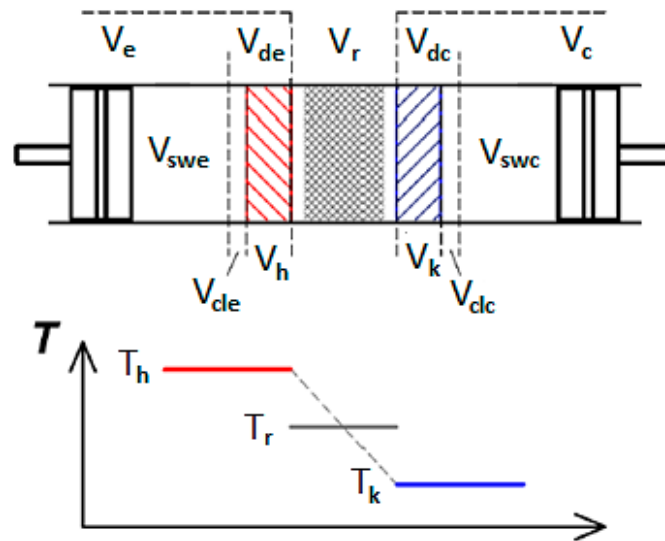


Figure 2. Schmidt analysis, adapted from [12].

According to these assumptions [13], the volumes are defined as:

$$V_e = V_{cle} + \frac{V_{swe}}{2} \cdot [1 - \cos(\varphi)] \quad (1)$$

For  $\alpha$ -type, the compression space is defined as:

$$V_c = V_{clc} + \frac{V_{swc}}{2} \cdot [1 - \cos(\varphi - \alpha_f)] \quad (2)$$

The main variables are pressure, volume, and temperature difference. When assessing efficiency in terms of temperatures, it is necessary to take into account the real possibilities and the technology available [14]. It is also necessary to adapt the maximum cycle temperatures to the pressure ratios and permissible operating pressures [15,16]. A slightly different condition in terms of heat transfer is achievable with the highest heater and lowest cooler temperatures—the highest determined by the heat source temperature and the lowest determined by the cooling method [17]. More advanced numerical model was presented by Urieli [18], with adiabatic engine assumptions. Another analytical model for estimating the performance of Stirling engines is known as finite speed thermodynamic analysis, which is based on the basic laws of thermodynamics. In last years the finite time thermodynamic analysis was used for an endoreversible Stirling engine [17].

To use the Stirling engine for waste heat recovery, the maximal temperature is determined by the source, in the form of gas, or liquid [19]. So it would seem most appropriate to use, or rather design a device with the highest possible mass flow to ensure sufficient power. Here, however, the opposite side of the problem must be realized. As the amount of working fluid flowing through the constant cross-section area or pipe increases, the speed increases, and the flow can become critical [20]. Thus, with increasing quantities, the entire volume must increase and the cost of the mechanical parts of the engine is disproportionately increasing as it is a piston machine. Other main reasons influencing the resulting cycle efficiency are harmful space of cylinders, low regenerator efficiency, real pressure losses in the regenerator, in pipes and heat exchangers, as well as mechanical friction losses of moving parts and also heat losses. The regenerator, as the main energy conservation part, has a significant role and the change in the inner heat transfer coefficient can influence total effectivity more than friction losses [21]. However, the regenerator quality can be also expressed in terms of enthalpy difference [22]. Our numerical model is based on [18] and adiabatic engine assumptions. According to the model, the engine is theoretically divided into five characteristic control volumes: expansion chamber (e), heater (h), cooler (k), regenerator (r), and compression chamber (k). The model is based on the basic

equations of mass and energy equilibrium, with a state equation applied to each control volume [18]. Figure 3 shows the general control volume and the relevant variables used in equations.

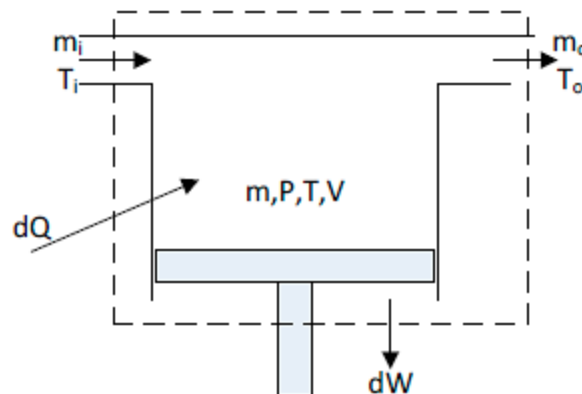


Figure 3. Common control volume [17].

By applying the mass balance equation to the above control volume, the mass change according to the piston crank position ( $\varphi$ ) can be expressed as:

$$\dot{m}_i - \dot{m}_o = \frac{dm}{d\varphi} \quad (3)$$

By including the equation of energy equilibrium and neglecting the kinetic components we get

$$\frac{dQ}{d\varphi} + c_{pi}T_i\dot{m}_i - c_{po}T_o\dot{m}_o = \frac{dW}{d\varphi} + c_v \frac{d(mT)}{d\varphi} \quad (4)$$

The evaluation of the pressure change in the engine operating space is calculated taking into account the mass balance applied to the whole engine.

$$M = m_c + m_k + m_r + m_h + m_e \quad (5)$$

And after supplying mass balance into the form of pressure equation:

$$p = \frac{Mr}{\frac{V_c}{T_c} + \frac{V_k}{T_k} + \frac{V_r}{T_r} + \frac{V_h}{T_h} + \frac{V_e}{T_e}} \quad (6)$$

The equation takes into account the pressure with the volume contained through the working fluid in each control volume. The volumes associated with the heater, cooler, and regenerator remain constant during the cycle. On the other hand, the volume in the compression and expansion spaces changes continuously and thus determines the pressure fluctuation during the cycle. Volume changes are determined by the dynamics of the crank mechanism, which determines the position of the pistons at different crank angle ( $\varphi$ ) values. These variations are considered sinusoidal and thus allow the derivation of different expressions for all engine configurations.

The expected temperature changes in the individual volumes are shown in Figure 4. Cooler and heater temperatures are assumed to be constant, with the temperatures of the compression and expansion spaces varying over the cycle depending on adiabatic expansion and compression. The compression and expansion work is calculated from the energy balance equation for the respective working volumes, which are considered adiabatic [18].

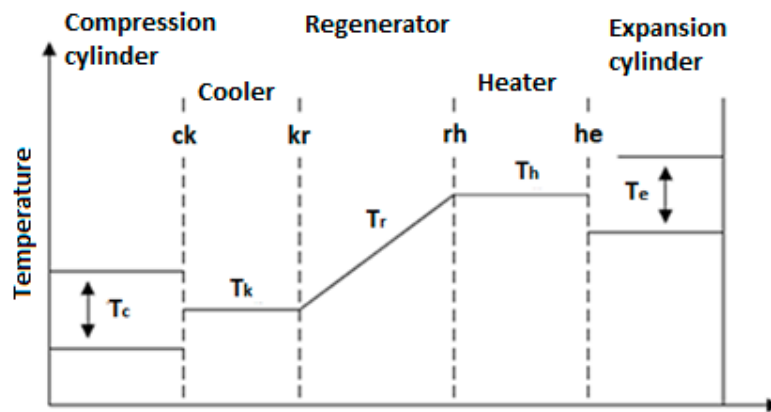


Figure 4. Temperature change in control volumes, adapted from [17].

Mass of working gas is defined by ideal isothermal Schmidt analysis. This analysis assumes isothermal working spaces, i.e., the temperatures in the compression and expansion space are equal to the temperatures of the cooler and heater [22–25]. These assumptions make it possible to obtain the following analytical expression.

$$M = \int_0^{2\pi} \frac{p}{r} \left( \frac{V_c}{T_k} + \frac{V_k}{T_k} + \frac{V_r}{T_r} + \frac{V_h}{T_h} + \frac{V_e}{T_h} \right) d\varphi \tag{7}$$

The analytical solution according to [17] for the alpaa configuration:

$$M = \frac{p_m (s \sqrt{1 - b^2})}{r} \tag{8}$$

where parameters “s” and “b” are defined as:

$$b = \frac{c}{s} \tag{9}$$

$$c = \frac{1}{2} \sqrt{\left( \frac{V_{swe}}{T_h} \right)^2 + 2 \frac{V_{swe}}{T_h} \frac{V_{swc}}{T_k} \cos(\alpha_f) + \left( \frac{V_{swc}}{T_k} \right)^2} \tag{10}$$

$$s = \frac{V_{swc}}{2T_k} + \frac{V_{clc}}{T_k} + \frac{V_k}{T_k} + \frac{V_r \ln \frac{T_h}{T_k}}{T_h - T_k} + \frac{V_h}{T_h} + \frac{V_{swe}}{2T_h} + \frac{V_{cle}}{T_e} \tag{11}$$

The working medium mass at each control volume and the mass flow rate at the control volume interfaces ( $m_{ck}$ ,  $m_{kr}$ ,  $m_{rh}$ ,  $m_{he}$ ) are evaluated at each crank angle position.

The mass components “j” representing the set  $j = \{k, r, h\}$  concerning the crank angle for heat exchangers, which are considered to be isothermal, are calculated from the equation:

$$\frac{dm_j}{d\varphi} = \frac{m_j}{p} \left( \frac{\partial p}{\partial \varphi} \right) \tag{12}$$

Mass components for compression and expansion volume, which are considered not to be isothermal, can be expressed as:

$$\frac{dm_c}{d\varphi} = \frac{p \left( \frac{\partial V_c}{\partial \varphi} \right) + \frac{V_c \left( \frac{\partial p}{\partial \varphi} \right)}{\kappa}}{r T_{ck}} \tag{13}$$

$$\frac{dm_e}{d\varphi} = \frac{p\left(\frac{\partial V_e}{\partial\varphi}\right) + \frac{V_e\left(\frac{\partial p}{\partial\varphi}\right)}{\kappa}}{rT_{he}} \quad (14)$$

Mass flow at each control volume boundary:

$$\dot{m}_{ck} = -\frac{\partial m_c}{\partial\varphi} \quad (15)$$

$$\dot{m}_{he} = -\frac{\partial m_e}{\partial\varphi} \quad (16)$$

$$\dot{m}_{kr} = \dot{m}_{ck} - \frac{\partial m_k}{\partial\varphi} \quad (17)$$

$$\dot{m}_{rh} = \dot{m}_{he} + \frac{\partial m_h}{\partial\varphi} \quad (18)$$

Furthermore, by substituting mass components into pressure change equation:

$$\frac{dp}{d\varphi} = -\frac{\kappa p\left(\frac{\partial V_c}{T_{ck}} + \frac{\partial V_e}{T_{he}}\right)}{\frac{V_c}{T_{ck}} + \kappa\left(\frac{V_k}{T_k} + \frac{V_r}{T_r} + \frac{V_h}{T_h}\right) + \frac{V_e}{T_{he}}} \quad (19)$$

The regenerator temperature change is linear and according to [22] can be defined as mean effective value:

$$T_r = \frac{T_h - T_k}{\ln\left(\frac{T_h}{T_k}\right)} \quad (20)$$

The temperature change for compression and expansion volume during the cycle can be expressed via a differential form of state equation for working gas:

$$\frac{dT_c}{d\varphi} = T_c\left(\frac{\partial p}{\partial\varphi} \frac{1}{p} + \frac{\partial V_c}{\partial\varphi} \frac{1}{V_c} - \frac{\partial m_c}{\partial\varphi} \frac{1}{m_c}\right) \quad (21)$$

$$\frac{dT_e}{d\varphi} = T_e\left(\frac{\partial p}{\partial\varphi} \frac{1}{p} + \frac{\partial V_e}{\partial\varphi} \frac{1}{V_e} - \frac{\partial m_e}{\partial\varphi} \frac{1}{m_e}\right) \quad (22)$$

Boundary temperatures  $T_{ck}$  and  $T_{he}$  are dependent on working medium flow direction.

By applying the energy balance equation to each heat exchanger, taking into account that these are isothermal spaces, we obtain, according to [18] the following expressions:

$$\frac{dQ_k}{d\varphi} = \frac{V_k\left(\frac{\partial p}{\partial\varphi}\right)c_v}{r} - c_p(T_{ck}m_{ck} - T_{kr}m_{kr}) \quad (23)$$

$$\frac{dQ_r}{d\varphi} = \frac{V_r\left(\frac{\partial p}{\partial\varphi}\right)c_v}{r} - c_p(T_{kr}m_{kr} - T_{rh}m_{rh}) \quad (24)$$

$$\frac{dQ_h}{d\varphi} = \frac{V_h\left(\frac{\partial p}{\partial\varphi}\right)c_v}{r} - c_p(T_{rh}m_{rh} - T_{he}m_{he}) \quad (25)$$

Compression and expansion work can be expressed from the energy balance equation for every control volume, which is considered as adiabatic:

$$\frac{dW_c}{d\varphi} = p \left( \frac{\partial V_c}{\partial \varphi} \right) \quad (26)$$

$$\frac{dW_e}{d\varphi} = p \left( \frac{\partial V_e}{\partial \varphi} \right) \quad (27)$$

Then the total cycle work, depending on the crank angle, is obtained as the sum of the individual components of the compression and expansion work.

$$\frac{dW}{d\varphi} = \frac{dW_c}{d\varphi} + \frac{dW_e}{d\varphi} \quad (28)$$

The system is solved as a quasi-static flow, so the mass flows in all control volumes (heater, cooler, regenerator) is constant for each integration interval. For the calculation, it is necessary to know at least the initial values of working temperatures for compression and expansion cylinder, which are the result of adiabatic processes and enthalpy flow. The only clue to their correct selection is that their end-of-cycle values should be equal to their respective values at the start of the cycle. The pressure variation in the working cylinder, according to Ipci and Karabulut [21], can be described as a function of temperature. Thermal resistance was also expressed according to Cheng [23]. Due to the cyclical nature of the system, the problem is solved by entering the initial conditions and integrating them over several cycles, with the optimization method based on [26–28]. The example calculation is performed for the Cleanergy C9G Stirling engine, using Matlab, partly the Matlab PDE toolbox [29]. Some solutions of differential equations were used according to [30]. Due to the model simplicity, one computational cycle took only few minutes to solve. Boundary conditions were established from experiments and from [31], where the same engine was examined. In this study [31], author examined fuel impact on engine effectivity and proved possible fuel change from natural gas to renewable sources.

In Figure 5 are presented the temperatures changes in the compression and expansion volumes during one cycle. The dashed lines represent the values of temperatures  $T_h$  and  $T_k$ , which represent a constant average value of the temperature of the heater and cooler heads, respectively. The  $T_e$  and  $T_c$  represent temperatures in expansion and compression volume. In this case, the values  $T_h = 313.15$  K,  $T_k = 973.15$  K, the mean value of the working pressure  $p_m = 150$  bar at the rotational frequency  $f = 25$  Hz were chosen. These values simulate the real operation of the device at the maximum pressure of the working medium. The temperatures of the expansion volume change in a wider temperature range, where the maximum absolute value of the change is equal to  $dT_e = 72.41$  K, while at a compression volume  $dT_c = 16.92$  K. This phenomenon is caused by the conversion of the thermal energy into mechanical energy. Energy change during one cycle is shown in Figure 6.

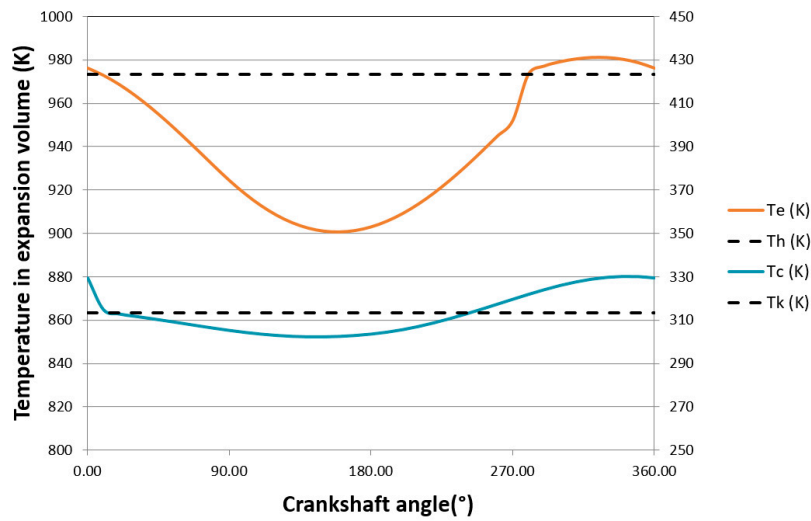


Figure 5. The temperatures during compression and expansion.

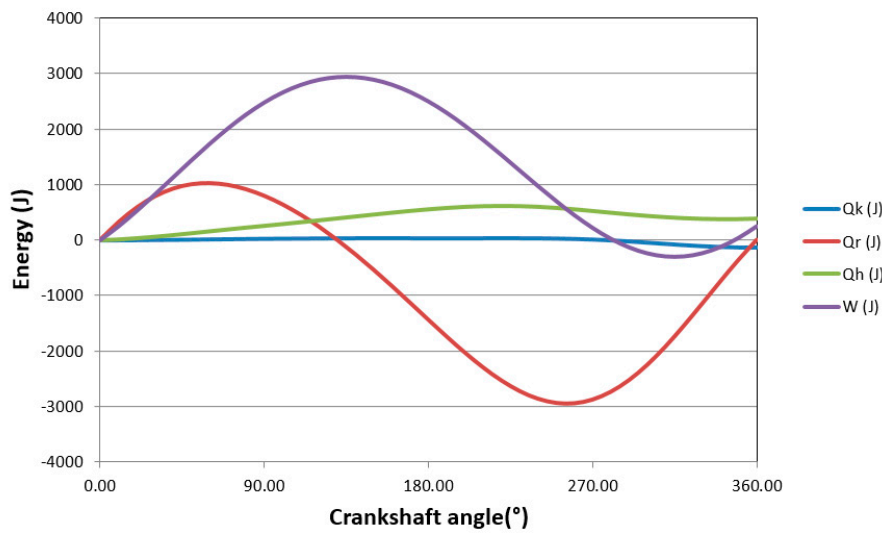


Figure 6. Energy change during one cycle.

### 3. Experimental Measurements

The measurement and calculation were made for the Stirling engine, which is part of the Cleanergy C9G cogeneration unit. The measurement was carried out at different engine operating pressure settings using natural gas as fuel. The layout is shown in Figure 7.

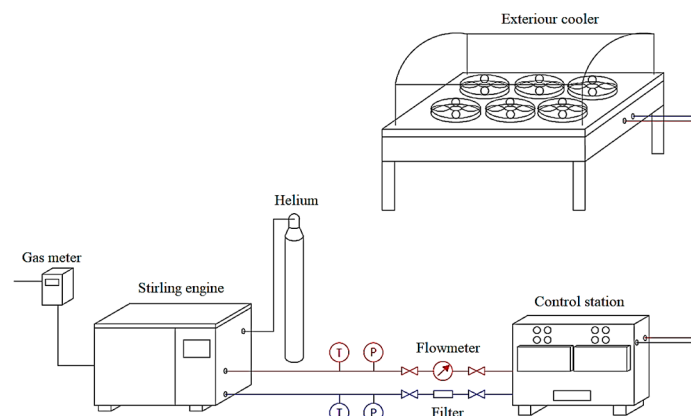


Figure 7. The experimental setup.

The measured parameters were the inlet and outlet temperature from the water heat exchanger, which is a part of the engine. To measure them, wells were created on the inlet and outlet pipes, in which the sensors were placed. Temperature measurements were performed with PT100 resistance thermometers, flow with magnetic flow meters, and pressure with pressure gauges. The internal engine parameters such as the temperature of the radiator, heater, combustion chamber, and helium working pressure are recorded by the engine control panel. These values are recorded on a computer using MODBUS technology. The cogeneration unit was connected to an exchanger control station, which cooled the excess thermal energy via an external cooler with a capacity of 50 kW. The working gas supply and the associated working gas pressure in the engine were provided by an electromagnetic valve located on the helium storage bottle. The electrical power produced was displayed on the control panel. Natural gas consumption was measured by a gas meter with remote reading.

The engine has its own control system, which allows to control and monitor the engine in real time, without computer connection. After pressing the start button, the control system checks working medium pressure, fuel gas pressure and starts to heat up the burning chamber. After reaching approx. 400 °C, the engine starts and continues the heating process until it reaches 520 °C in the combustion chamber, when the engine starter disconnects and the engine starts to produce electricity. After few test experiments we have found out, that there is a huge difference between hot and cold start. For cold start, where the engine and cooling circuit have ambient temperature, the heating process lasts at least 15 min, electricity is produced after 7 min and after another 8 min the electricity production is stable. For a hot start, where cooling circuit is pre-heated to 80 °C and engine is not cooled down, with hot cylinder temperature of 200 °C, the starting process took only 7 min, where electricity production occurred after 1.5 min. Due to this we have always started the measurement with cold engine, with cooled down heating circuit. Every experiment consisted of 4 periods—starting process, engine pressure setup, measurement, cooling down. The main measurement was performed for 2 h, under stable conditions, where data were collected via ModBus: engine working pressure, engine heater temperature, engine cooler temperature, electric output at generator, external cooling system temperatures and mass flow. From these data, the average value was expressed and standard deviation estimation was determined, according to [31–33], as:

$$\bar{x} = \frac{1}{n} \sum_{i=1}^n x_i \quad (29)$$

$$s_{\bar{x}} = \sqrt{\frac{\sum_{i=1}^n x_i^2 - n\bar{x}^2}{n(n-1)}} \quad (30)$$

where  $n$  is the number of measured values, in our case it is 360,  $x_i$  is the measured value and  $s_{\bar{x}}$  is standard deviation.

For indirect measured values, standard deviation was determined according to [31–33] as:

$$s_y^2 = \sum_{i=1}^n \left( \frac{\partial y}{\partial x_i} s_i \right)^2 \quad (31)$$

The results of measurement and standard deviation of the arithmetic mean value estimation are presented in the Table 2. These results served as sample for comparison with proposed numerical model.

**Table 2.** Measured electric output with standard deviation.

Working Pressure (bar)	Electric Output—Average Value (W)	Efficiency (%)	Standard Deviation of the Arithmetic Mean Value Estimation (W)
48.2	2480	16.7	±6.5
52.1	2730	17.1	±4.8
56.3	2990	17.6	±5.8
59.9	3240	18.8	±4.1
65	3510	19.5	±4.9
70	3820	20.0	±5.0
80.9	4060	20.9	±5.7

### 4. Results

The experiments were made with working medium pressure from 48 to 81 bar. The measured data were subsequently compared with the results of the numerical model. The results are shown in Figure 8. Net power represents electrical output measured on electric generator. The comparison shows quite good accuracy, with error from 2% to 8%, and proved, that the model is suitable for prediction with other working conditions, in this case with heat recovery system as a heat source.

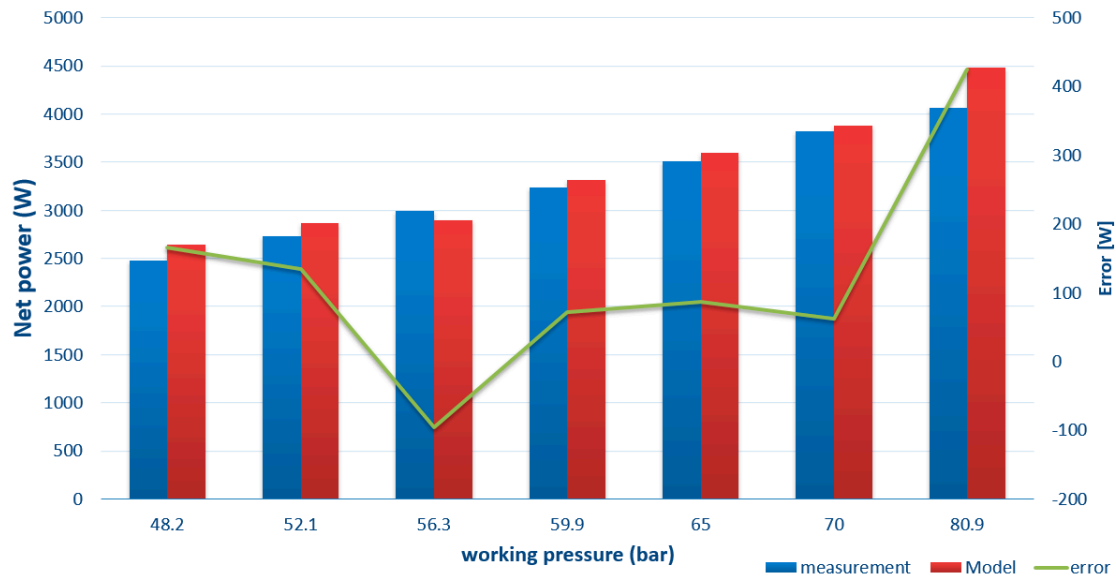


Figure 8. The comparison of the numerical model and experimental data.

To visualize the changes and dependencies, we have also chosen to create a p-V diagram for different mean working pressures of the engine. Figure 9 shows the dependence of the working pressure on the volume at the cooler temperature  $T_k = 313.15$  K, the heater temperature  $T_h = 973.15$  K, and the frequency  $f_m = 25$  Hz.

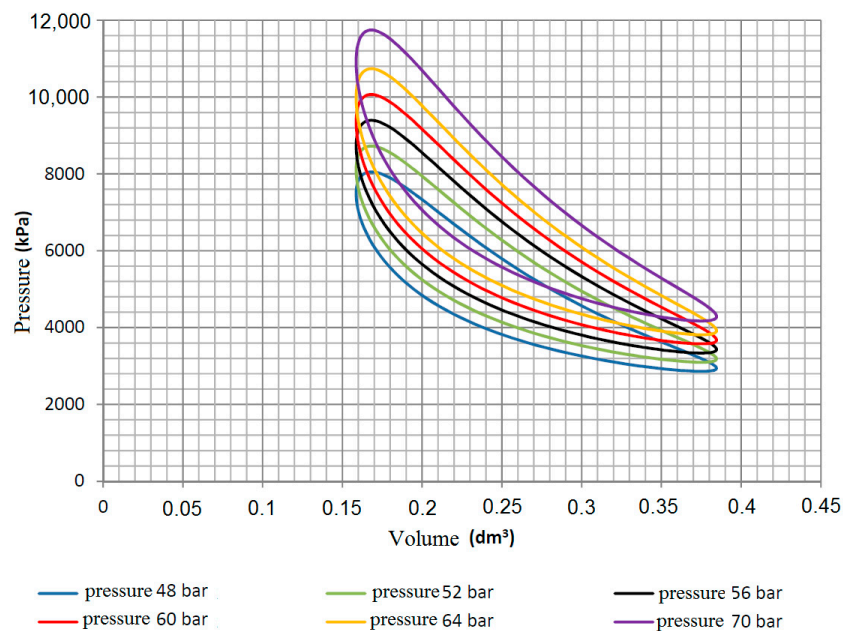


Figure 9. P-V diagram for different mean working pressure.

With the increasing pressure of the working medium the increase in the heat capacity is present, so an increase in heat flow, which has a positive effect on the overall performance of the cycle. This change can be best shown in p-V diagram, where the area is expanding according to raising pressure of working medium, as shown in Figure 9.

As the main characteristic parameter of waste heat is the temperature of stream, for example of flue gases, or radiating surfaces temperature. We decided to take the temperature of the heat source as the main variable for our Cleanergy engine model. Net efficiency, for various pressures, is shown in next Figure 10. Variable was working pressure, with constant heater temperature of 550 °C.

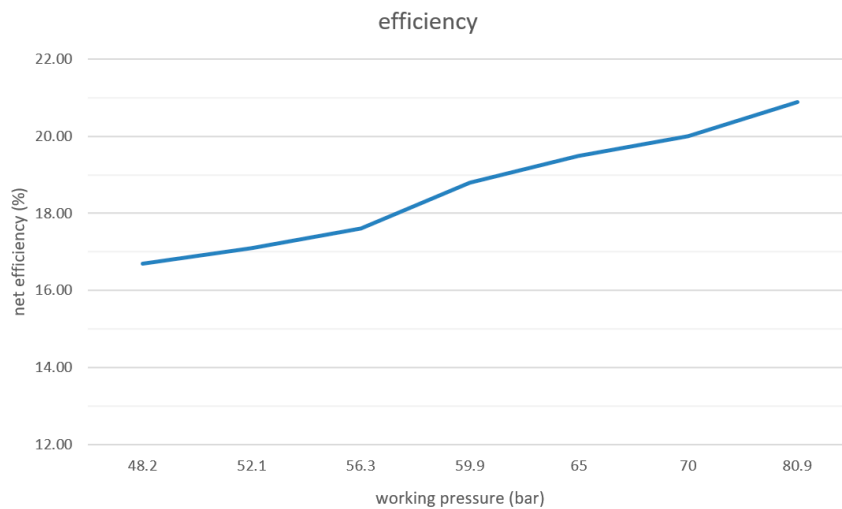


Figure 10. Net efficiency.

The numerical simulation with heat source temperatures varying from 300 °C to 800 °C and with working medium pressure from 15 to 90 bar was also carried out. The results are shown in Figure 11.

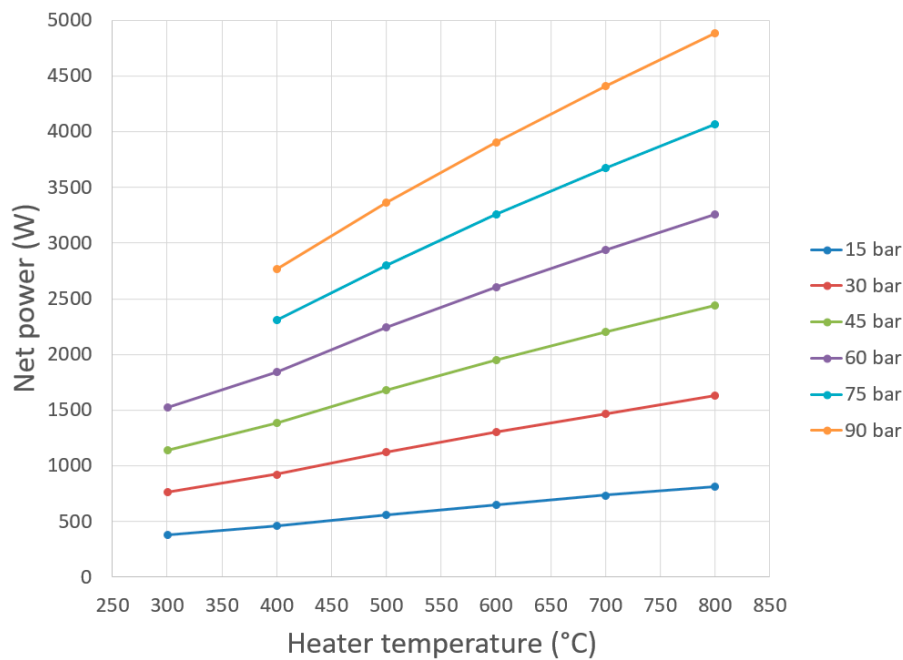


Figure 11. The numerical simulation for different pressures and heater temperatures.

## 5. Discussion

Several experimental tests were done and this Cleanergy engine, as many kinetic engines, showed flexibility at various pressures and temperatures. For lower pressures, the 15 and 30 bar, the engine showed only small impact of temperature at net power, due to the pressure drop in exchangers, which was also mentioned in [23]. The proposed numerical model, based on [22] and [23] was adapted to the existing Stirling engine, the Cleanergy engine. Regenerator properties were adapted according to [18], which in the final led to an error from 2% to 8% in comparison to experimental measurements. The numerical simulations of the engine were done with various working mediums, pressures, and temperatures. The results are shown in previous figures, where the lowest heater temperature, at which the engine still works, is predicted at 300 °C. This is in the medium temperature range and therefore this kind of engine can be capable to recover heat from industrial applications, such as heavy industry, exhaust heat but also for solar concentrating systems.

## 6. Conclusions

The aim of this work is to give information from experiments with this commercially available engine under various conditions and its capability for the heat recovery system. Measurements were made with different working pressures and served as basis for proposed simplified numerical model. The numerical model was later updated to describe this particular engine under wider circumstances and to show the potential use of this engine. Analysis showed strong dependence of this engine from heater temperature for higher working medium pressures, where with constant pressure the electric output of whole unit can be doubled with growing temperature. Working medium pressure from certain level has even bigger impact, where under constant heater temperature with rising pressure power output rises quasi linearly. This analysis showed that this engine should be capable of utilizing heat from 300 °C. For lower temperatures, numerical model was unstable and predicted zero power output. Therefore, it is assumed that this engine can be used for medium range waste heat, around 300 °C, for heat recovery from industrial applications or for use with renewable energy sources, for example with solar concentrating power systems. To use a Stirling engine for low potential heat, we have to look for other configurations or alternatives as this kind of engine. Two large Stirling engine groups, thermoacoustic and free-piston engines, are not so interesting due to the higher costs and technological difficulty. Stirling engines with liquid pistons can operate at very low temperatures but have a power output of only several watts.

**Author Contributions:** Conceptualization, P.D. and R.N.; writing—review and editing, P.D.; funding acquisition J.J. All authors have read and agreed to the published version of the manuscript.

**Funding:** This research is supported by the project “Influence of combustion conditions on the production of solid pollutants in small heat sources”, VEGA 1/0479/19. This research is supported by the project VEGA-1/0738/18, Optimization of energy inputs for the rapid generation of natural gas and biomethane hydrates for the accumulation of high potential primary energy “. This work is supported by “Research of new ways of converting heat from RES to electricity using new progressive cycles” ITMS 26220220117.

**Conflicts of Interest:** The authors declare no conflict of interest.

## Nomenclature, Abbreviations

Symbol	Unit	Description
$m$	(kg)	working gas mass
$\dot{m}$	(kg)	mass flow
$M$	(kg)	total weight of the engine working medium
$Q$	(J)	heat added or removed
$T$	(K)	temperature
$V$	(m)	volume
$W$	(J)	work

$V_{swc}$	(m <sup>3</sup> )	compression cylinder displacement
$V_{swe}$	(m <sup>3</sup> )	expansion cylinder displacement
$\dot{m}_{he}$	(kg/s)	mass flow through heater to expansion cylinder interface
$\dot{m}_{ck}$	(kg/s)	mass flow through compression cylinder to cooler interface
$\dot{m}_{kr}$	(kg/s)	mass flow through cooler to regenerator interface
$\dot{m}_{rh}$	(kg/s)	mass flow through regenerator to heater interface
$\dot{m}_i$	(kg/s)	mass flow entering the control volume
$\dot{m}_o$	(kg/s)	mass flow exiting the control volume
Index		
$c$		compression volume, cylinder
$e$		expansion volume, cylinder
$h$		heater
$k$		cooler, cooling volume
$r$		regenerator

## References

- Holland, D. *An Introduction to Stirling-Cycle Machine*, Stirling-Cycle Research Group; Department of Mechanical Engineering, University of Canterbury: Christchurch, New Zealand, 2012.
- Renzi, M.; Brandoni, C. Study and application of a regenerative Stirling cogeneration device based on biomass combustion. *Appl. Therm. Eng.* **2014**, *67*, 341–351. [[CrossRef](#)]
- Invernizzi, C.M. *Closed Power Cycles*; Springer: London, UK, 2013; ISBN 978-1-4471-5140-1.
- Thombare, D.G.; Verma, S.K. Technological development in the Stirling cycle engines. *Renew. Sustain. Energy Rev.* **2008**, *12*, 1–38. [[CrossRef](#)]
- McGovern, J.; Cullen, B.; Feidt, M.; Petrescu, S. Validation of a Simulation Model for a Combined Otto and Stirling Cycle Power Plant. Presented at ASME 4th International Conference on Energy Sustainability, Phoenix, AZ, USA, 17–22 May 2010.
- Finkelstein, T.; Organ, A.J. *Air Engines: The history, Science, and Reality of Perfect Engine*; ASME Press: New York, NY, USA, 2001; ISBN-13: 978-07918-0171-0.
- Wang, K.; Sanders, R.S.; Dubey, S.; Choo, F.H.; Duan, F. Stirling cycle engines for recovering low and moderate temperature heat: A review. *Renew. Sustain. Energy Rev.* **2016**, *62*, 89–108. [[CrossRef](#)]
- Araoz, J.A.; Salomon, M.; Alejo, L.; Fransson, T.H. Numerical simulation for the design analysis of kinematic Stirling engines. *Appl. Energy* **2015**, *159*, 633–650. [[CrossRef](#)]
- Karabulut, H.; Cinar, C.; Ozturk, E.; Yucesu, H. Torque and power characteristics of a helium charged Stirling engine with a lever controlled displacer driving mechanism. *Renew. Energy* **2010**, *35*, 138–143. [[CrossRef](#)]
- Kwankaomeng, S.; Silpsakoolsook, B.; Savangvong, P. Investigation on stability and performance of a free-piston Stirling engine. *Energy Procedia* **2014**, *52*, 598–609. [[CrossRef](#)]
- Cooke-Yarborough, E.H. *A Proposal for a Heat-Powered Non-Rotating Electrical Alternator*; UKAEA Atomic Energy Research Establishment: Harwell, UK, 1967.
- Martini, W.R. *Stirling Engine Design Manual*, 2nd ed.; University Press of the Pacific: Honolulu, HI, USA, 2004; ISBN 1-4102-1604-7.
- Hirata, K. *Schmidt Theory for Stirling Engines*; National Maritime Research Institute: Tokyo, Japan, 1997.
- Charvát, P.; Klimeš, L.; Pech, O.; Hejčík, J. Solar air collector with the solar absorber plate containing a PCM—Environmental chamber experiments and computer simulations. *Renew. Energy* **2019**, *143*, 731–740.
- Nemec, P.; Caja, A.; Malcho, M. Mathematical Model for Heat Transfer Limitations of Heat Pipe. *Math. Comput. Model.* **2013**, *57*, 126–136. [[CrossRef](#)]
- Chen, L.; Li, J.; Sun, F. Optimal temperatures and maximum power output of a complex system with linear phenomenological heat transfer law. *Therm. Sci.* **2009**, *13*, 33–40. [[CrossRef](#)]
- Hosseinpour, J.; Sadeghi, M.; Chitsaz, A.; Ranjbar, F.; Rosen, M.A. Exergy assessment and optimization of a cogeneration system based on a solid oxide fuel cell integrated with a Stirling engine. *Energy Convers. Manag.* **2017**, *143*, 448–458. [[CrossRef](#)]
- Urieli, I.; Berchowitz, D.M. *Stirling Cycle Engine Analysis*; Taylor & Francis: Ann Arbor, MI, USA, 1984; 256p, ISBN 0852744358.

19. Ferreira, A.C.; Nunes, M.L.; Teixeira, J.C.; Martins, L.A.; Teixeira, S.F. Thermodynamic and economic optimization of a solar-powered Stirling engine for micro-cogeneration purposes. *Energy* **2016**, *111*, 1–17. [[CrossRef](#)]
20. Chen, W.L.; Wong, K.L.; Chen, H.E. An experimental study on the performance of the moving regenerator for a gamma-type twin power piston Stirling engine. *Energy Convers. Manag.* **2014**, *77*, 118–128. [[CrossRef](#)]
21. Ipci, D.; Karabulut, H. Thermodynamic and dynamic analysis of an alpha type Stirling engine and numerical treatment. *Energy Convers. Manag.* **2018**, *169*, 34–44. [[CrossRef](#)]
22. Cheng, C.-H.; Yu, Y.-J. Numerical model for predicting thermodynamic cycle and thermal efficiency of a beta-type Stirling engine with rhombic-drive mechanism. *Renew. Energy* **2010**, *35*, 2590–2601. [[CrossRef](#)]
23. Cheng, C.-H.; Tan, Y.-H. Numerical optimization of a four-cylinder double-acting stirling engine based on non-ideal adiabatic thermodynamic model and scgm method. *Energies* **2020**, *13*, 2008. [[CrossRef](#)]
24. Brestovič, T.; Carnogurska, M.; Prihoda, M.; Lukac, P.; Lázár, M.; Jasminská, N.; Dobáková, R. Diagnostics of hydrogen-containing mixture compression by a two-stage piston compressor with cooling demand prediction. *Appl. Sci.* **2018**, *8*, 625. [[CrossRef](#)]
25. Világi, F.; Knížat, B.; Mlkvik, M.; Urban, F.; Olšiak, R.; Mlynár, P. Mathematical model of steady flow in a helium loop. *Mech. Ind.* **2019**, *20*, 704–712.
26. Ahmed, F.; Hulin, H.; Khan, A.M. Numerical modeling and optimization of beta-type Stirling engine. *Appl. Therm. Eng.* **2019**, *149*, 385–400. [[CrossRef](#)]
27. Ni, M.; Shi, B.; Xiao, G.; Peng, H.; Sultan, U.; Wang, S.; Luo, Z.; Cen, K. Improved Simple Analytical Model and experimental study of a 100W  $\beta$ -type Stirling engine. *Appl. Energy* **2016**, *169*, 768–787. [[CrossRef](#)]
28. Bataineh, K.M. Numerical thermodynamic model of alpha-type Stirling engine. *Case Stud. Therm. Eng.* **2018**, *12*, 104–116. [[CrossRef](#)]
29. Rogdakis, E.D.; Antonakos, G.D.; Koronaki, I.P. Thermodynamic analysis and experimental investigation of a Solo V161 Stirling cogeneration unit. *Energy* **2012**, *45*, 503–511. [[CrossRef](#)]
30. Westerberg, J. An Experimental Evaluation of Low Caloric Value Gaseous Fuels as a Heat Source for Stirling Engines. Master's Thesis, Chalmers University of Technology, Goteborg, Sweden, March 2014.
31. Wackerly, D.; Mendenhall, W.; Scheaffer, R.L. *Mathematical Statistics with Applications*, 7th ed.; Thomson Brooks/Cole: Pacific Grove, CA, USA, 2008; ISBN-13: 978-0495110811.
32. Sarkar, J.; Rashid, M. Visualizing Mean, Median, Mean Deviation, and Standard Deviation of a Set of Numbers. *Am. Stat.* **2016**, *70*, 304–312. [[CrossRef](#)]
33. Pobočková, I.; Sedliačková, Z.; Michalková, M. Application of Four Probability Distributions for Wind Speed Modeling. *Procedia Eng.* **2017**, *192*, 713–718. [[CrossRef](#)]



© 2020 by the authors. Licensee MDPI, Basel, Switzerland. This article is an open access article distributed under the terms and conditions of the Creative Commons Attribution (CC BY) license (<http://creativecommons.org/licenses/by/4.0/>).